UC Irvine
UC Irvine Previously Published Works

Title

Experimental study of a plasma-filled backward wave oscillator

Permalink

https://escholarship.org/uc/item/2tr0d2tn

Journal

IEEE Transactions on Plasma Science, 21(1)

ISSN

0093-3813

Authors

Zhai, X
Garate, E
Prohaska, R
et al.

Publication Date

1993

DOI

10.1109/27.221113

Peer reviewed

Experimental Study of a Plasma-Filled Backward Wave Oscillator

Xiaoling Zhai, Eusebio Garate, Robert Prohaska, Gregory Benford, and Amnon Fisher, *Member IEEE*

Abstract— We present experimental studies of a plasma-filled X-band backward wave oscillator (BWO). Depending on the background gas pressure, microwave frequency upshifts of up to 1 GHz appeared along with an enhancement by a factor of 7 in the total microwave power emission. The bandwidth of the microwave emission increased from $\leq$ 0.5 GHz to 2 GHz when the BWO was working at the rf power enhancement pressure region. The rf power enhancement appeared over a much wider pressure range in a high beam current case (10–100 mT for 3 kA) as compared to a lower beam case (80–115 mT for 1.6 kA). The plasma-filled BWO has higher power output compared to the vacuum BWO over a broader region of magnetic guide field strength. Trivelpiece–Gould modes (T–G modes) are observed with frequencies up to the background plasma frequency in a plasma-filled BWO. Mode competition between the Trivelpiece–Gould modes and the X-band TM$_{01}$ mode prevailed when the background plasma density was below 6×10^{11} cm^{-3}. At a critical background plasma density of $n_{cr} \cong 8 \times 10^{11}$ cm^{-3} power enhancement appeared in both X-band and the T–G modes. Power enhancement of the S-band in this mode collaboration region reached up to 8 dB. Electric fields measured by the Stark-effect method were as high as 34 kV/cm while the BWO power level was 80 MW. These electric fields lasted throughout the high power microwave pulse.

I. INTRODUCTION

INTENSE relativistic electron beam excitation of slow wave structures has been an active subject since Nation [1] confirmed the possibility in 1972. Many vacuum slow wave devices have been studied [2]–[6] since, with conversion efficiency of beam kinetic energy into microwaves as high as 30%. Using current pulse power technology, vacuum backward wave oscillators (BWO's) can emit microwave power as high as 1 GW [7]–[8]. Injecting plasma into the slow wave structure [9]–[11] enhances power emission by factors of 3 to 8, however, the basic mechanism is not well understood. All previous plasma-filled BWO experiments concentrated on producing higher power microwaves, higher efficiency and longer pulses. This work studies (a) the effect background plasma has on microwave frequency f and bandwidth Δf; (b) the plasma modes (Trivelpiece–Gould modes) in the plasma-filled BWO and their effect on the BWO waveguide mode (TM$_{01}$); and (c) measuring the electric field properties in the plasma-filled BWO through the atomic light emission (spectroscopic method).

Filling a slow wave supporting structure with plasma modifies its original dispersion characteristics. The presence of the plasma allows propagation of electromagnetic (EM) waves with frequency below the plasma frequency, f_p, the Trivelpiece–Gould (T–G) modes [12]. A recent calculation [13] analyzed the low frequency modes in a plasma-filled BWO. Of particular interest in this calculation were modes that could axially bunch the electron beam so that stimulated electromagnetic emission could occur. Analyzing electron beam coupling to the modes showed instability for a dense set of frequencies below the plasma frequency, f_p. In addition to the T–G modes of the system, the plasma-filled BWO supports EM waves with $f > f_p$, which can axially bunch the electron beam. These are the usual TM$_{0n}$ modes of the plasma-filled BWO system, modified by addition of the plasma [14]. The TM$_{01}$ mode of the plasma-filled BWO is the mode for which enhanced power output has been previously observed [9]–[11]. It has been suggested that the T–G modes could play an important role [14] in the TM$_{01}$ mode power enhancement. We previously reported [15] detection of T–G modes in a plasma filled BWO, and the correlation between T–G modes and the BWO TM$_{01}$ mode.

Plasma can also affect the BWO rf spectrum. A recent theoretical description of the plasma-filled BWO [16] showed that the addition of plasma results in a frequency upshift in the output of the BWO, the amount of shift depending on the plasma density, n_p. An upshift up to 2.5 GHz was predicted for $n_p = 8 \times 10^{11}$ cm^{-3} for the BWO geometry considered (same as our BWO geometry) with no information about how bandwidth changes with plasma density. Our experimental measurement [12] indicated an upshift of about 1 GHz at $n_p = 8 \times 10^{11}$ cm^{-3}.

Behavior of the electric field in the plasma filled BWO, in a region where the relativistic electron beam, high power rf and plasma interact, could add important information for understanding the basic mechanisms of plasma-filled slow wave devices. To measure the electric field in the center of the BWO, spectroscopic methods can be employed. This method will not interfere with the basic interaction mechanisms, and the high level electromagnetic noise will not affect the measurement. In this paper, we also present results of spectroscopic measurement of the electric field in the plasma filled BWO.

II. EXPERIMENTAL SETUPS

In our experiment (Fig. 1), a Marx capacitor bank generates a 650 kV, 2 kA voltage pulse with 500 ns pulse duration. The electron beam was produced by field emission from a graphite-

1. Anode   2. Cathode
3. Reflector   4. BWO
5. Shunt resistor 6. Beam dump
7. Helium inlet 8. Magnetic coils
9. rf receiving horn 10. Attenuator
11. 8 channel X-band rf spectrometer
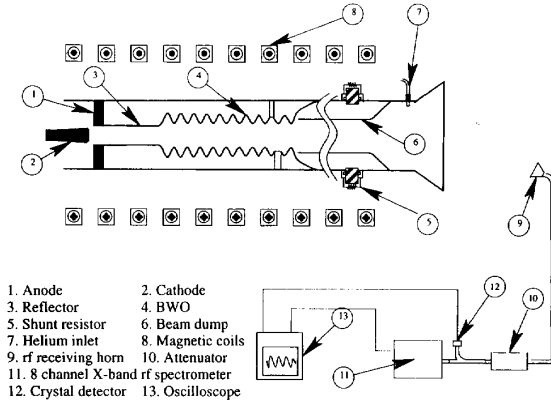12. Crystal detector 13. Oscilloscope

Fig. 1. Experimental setup.

cathode. The beam is annular with 1.8 cm diameter and 2 mm thickness, and is injected into the BWO along a guiding magnetic field. The BWO is a cylindrical waveguide with a periodically varying wall radius, $R(z)$, sinusoidally rippled about the mean radius, R_0, such that

$$R(z) = R_0 + h\cos(k_0 z)$$

$$k_0 = 2\pi/z_0 \tag{1}$$

where $h = 0.45$ cm is the ripple amplitude, $z_0 = 1.67$ cm is the period, and $R_0 = 1.45$ cm. (This BWO copies that of the University of Maryland [10], [14] experiments.) Beam current and voltage were monitored near the cathode, with down stream current measured by a shunt resistor. The BWO was immersed in a 6–18 kG guiding magnetic field. An X-band horn placed 2 m from the end of the drift tube received the microwave emission from the BWO. The microwaves were guided through 20 m of X-band waveguide into a screen room. Here the microwaves were measured by a crystal detector and an X-band 8 channel microwave spectrometer, covering 8.2 GHz $< f <$ 12.4 GHz. Each channel had a bandwidth of approximately 0.5 GHz. The spectrometer filters had 50 dB stopband insertion loss with 0.9 dB passband insertion loss.

Our window for the spectroscopic measurement (Fig. 2) was on the ninth ripple of the BWO (total ten ripples). We used two lenses to image the photons from the BWO center to the optical fibers. The first, with a short focal length, focused light from the center to the second lens. The second lens, with a much longer focal length, focused light to the optical fibers. This setup was chosen to match the f-number of the optical fibers. Two optical fibers transferred the light to a screen room 20 m away from the source. Both fibers were silicon, which has high efficiency and doesn't produce much light when hit by background X-rays. A 1 mm core diameter fiber looked at the allowed line $\lambda = 501.56$ nm from the helium (we used helium plasma). To improve light gathering efficiency for the forbidden lines we used a liner bundle consisting of 50 small fibers with 200 mm diameter. The end near the light source was circular with 1.6 mm diameter, and the other end was a 12 mm long array to match the entrance slit of the monochromator. Both monochromators had a holographic blazed grating with 1800 grooves/mm;

the reciprocal linear dispersion of the instrument was 0.7 nm/mm. The detectors were two Hamamatsu R 1894 and R 1635 photomultiplier tubes, both with 0.8 ns rise time. Outputs from the photomultiplier tubes were then recorded by a Tektronix DSA 602 Digitized oscilloscope (1 Gs/s). To prevent systematic error, the spectroscopic system was calibrated daily with a helium discharge lamp. In order to be sure that only the helium emission could be recorded by the photomultiplier, we tuned the two monochromators to the helium allowed and forbidden lines with no helium in the system, and got less than a total of 10 photons over more than 20 shots.

The observation window was also used for the T–G mode measurement. A coaxial cable extended through one window into the BWO with the center conductor acting as a microwave antenna (Fig. 3). Microwaves went through more than 30 m of RG-9 cable, which attenuates the rf signal at 0.7 dB/m for 4 GHz and ∼1 dB/m for 9 GHz. Low frequency microwaves were measured with a crystal detector, or with 8 channel S-band (2.6 GHz $< f <$ 3.9 GHz) and J-band (5.85 GHz$< f <$ 8.2 GHz) microwave spectrometers. Each channel of the S-band spectrometer covered approximately 160 MHz bandwidth with the J-band channels covering approximately 294 MHz bandwidth. In both microwave spectrometers the filters had 50 dB stopband insertion loss with 0.9 dB passband insertion loss. We measured frequencies between 3.9 GHz and 5.85 GHz with high pass filters (right circular cylinders with holes drilled along the axis; the hole radius determined the cut-off frequency), since we had no C-band spectrometer. Frequency-resolved measurements below 2.6 GHz were not made due to lack of diagnostic equipment.

Fig. 4 is the experimental setup for the plasma density measurement. We choose helium plasma because of its simple spectrum which also made the spectroscopic measurement easier. Plasma was produced by background helium gas ionization from the electron beam. As shown in Fig. 1, helium gas was injected from one end of the drift chamber and pumped out by the diffusion pump at the other end. Adjusting the helium inlet valve and the pumping speed maintained the helium pressure in the BWO at a constant of a few mT to 150 mT. The injected electron beam produced plasma by beam impact ionization, with $n_p(t)$ adjusted by controlling the gas pressure in the chamber. To measure the plasma density, we used a 10 kW, 4 μs pulse duration, 9.6 GHz X-band magnetron as the rf source. In order to avoid strong X-band TM$_{01}$ radiation and to not modify the oscillator, we replaced our BWO with a stainless steel tube of 10 mm radius, keeping anode and cathode geometry the same. Since the X-band radiation consistently arrived 140 ns (± 10 ns) into the beam pulse, we could correlate the microwave signal with the plasma density measurement at the turn on of the microwaves. However, this measurement most likely underestimates the plasma density during the high power rf emission. The magnetron rf was fed through the plasma by X-band waveguide, carrying information about plasma density $n_p(t)$ in its phase change $\Delta f(t)$. The probe rf was fed through an X-band bandpass filter (8.2 GHz–12.4 GHz) to limit the noise from beam radiation, then it was mixed with rf from
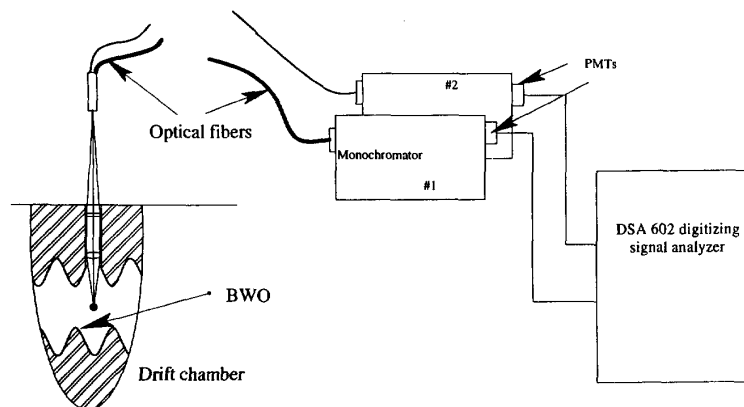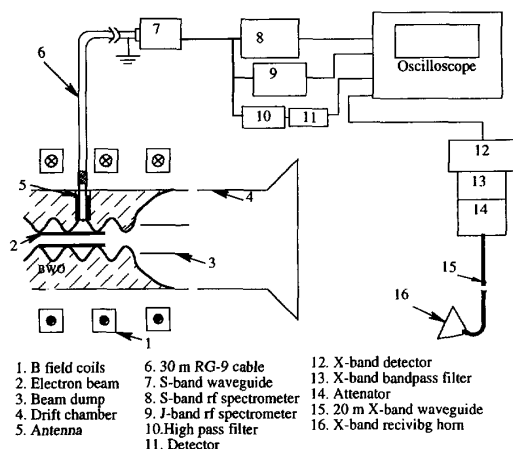
Fig. 2. Spectroscopic system.

1. B field coils	6. 30 m RG-9 cable	12. X-band detector
2. Electron beam	7. S-band waveguide	13. X-band bandpass filter
3. Beam dump	8. S-band rf spectrometer	14. Attenator
4. Drift chamber	9. J-band rf spectrometer	15. 20 m X-band waveguide
5. Antenna	10.High pass filter	16. X-band recivibg horn
	11. Detector	

Fig. 3. Experimental setup for Trivelpiece–Gould modes measurement.

a local oscillator so that a mixed frequency of ~ 100 MHz was obtained. The phase shift $\Delta f(t)$ occurs in the frequency difference $f_M(t) = f_{magnetron} - f_{oscillator}$ as a frequency change $\Delta f_M(t)$. $\Delta f(t)$ can be obtained by comparing this new frequency to the unshifted mixed frequency $f_{M0} = f_M(t < t_0, t_0$ is the beam start time), so that $\Delta f_M(t) = f_M(t) - f_{M0}$. We used this method, rather than a conventional interferometer, where one source is needed, to avoid high levels of broadband X-band noise from the electron beam. The heterodyne technique and the large magnetron input power circumvented this problem by allowing us to use high attenuation in the detector arm. With no plasma in the system, we detected no shift in the frequency difference Δf_{M0}, for up to 3 μs. The beam voltage pulse was synchronized with the stable portion of the mixed frequency. The results of this measurement are presented in Fig. 5.

III. EXPERIMENTAL RESULTS AND DISCUSSION

A. Dependency of rf Power and Spectrum on the Plasma Density

This experimental investigation of the plasma-filled BWO started with studying the effect of plasma on the BWO microwave power output level and microwave spectrum. First, we measured the vacuum BWO rf output. Fig. 6(a) shows the beam voltage and the eight channel X-band microwave spectrometer signals from the vacuum BWO for 3 kA beam current. In the vacuum BWO rf signal appeared ~ 140 ns after the beam turned on, this time delay was independent of the beam current for $I = 3$ kA, 2 kA, and 1.6 kA. Microwave output was always in the first channel of the spectrometer (8.2 to 8.725 GHz, 8.46 GHz center frequency). Maximum power emission was about 80 to 100 MW with microwave pulse duration of 50 ns (FWHM). We calculated the rf power by measuring the power angular distribution, then integrating overall space. Considering our beam pulse was 500 ns, the 50 ns rf pulse was very short. However, when the BWO operated at lower level powers, the microwave emission lasted longer. For example, microwave radiation with power output of 30–40 MW lasted between 130 ns and 150 ns.

As helium was added to the device, we observed a change in the BWO rf power output level and the rf spectrum, but the rf pulse still appeared at ~ 140 ns into the beam pulse. At low gas pressure (under 10 mT) and $I = 3$ kA only channel 1 and 2 of the spectrometer detected microwaves. However, in the pressure region of rf power enhancement (50 mT $< P_{He} <$ 80 mT), signals appeared in the first four channels of the spectrometer. It is interesting to note that the signal in channel 1 was never less than the vacuum BWO output level, and actually its output was the largest among all channels when the background helium pressure was below 25 mT. When the helium pressure was between 25 mT and 50 mT, rf signals appeared in the first three channels of the spectrometer, and the signal amplitude in the second and third channel increased to the same level as the first channel. At the pressure for maximum power, the third channel detected the largest signal. This indicted a frequency upshift of 1 GHz. Fig. 6(b) shows a shot taken at 60 mT with 3 kA beam current. If we sum the signal output from all channels of the spectrometer in Fig. 6(b) and compare to the signal in Fig. 6(a), it is more than seven times larger. Comparison also shows the bandwidth, Δf, increased from ≤ 0.5 GHz in vacuum to 2 GHz. We observed similar frequency upshift and bandwidth increase for the 1.6 kA case as well. Microwave emission bandwidth as a function
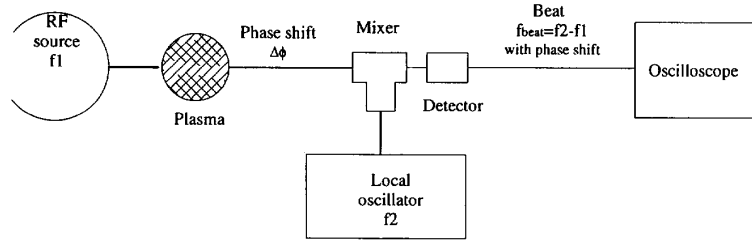
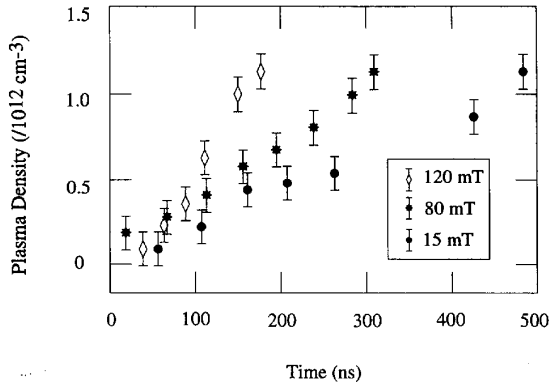Fig. 4. Experimental setup for the plasma density measurement.

Fig. 5. Plasma density as a function of time for three different helium pressures. Beam start at $t = 0$, and beam current is 1.6 kA. The rf pulse in the BWO arrives at $t \sim 140$ ns. This is likely an underestimate of the plasma density in the BWO since there is no high power rf.
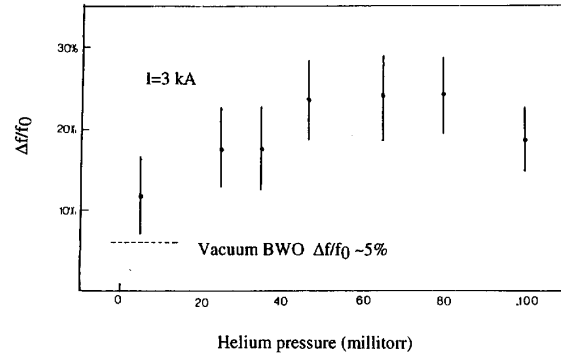

Fig. 7. Bandwidth of the microwave pulses vs. background helium pressure. Δf is the frequency range of microwave output, f_0 is the vacuum rf center frequency. Error is about $\pm 5\%$ due to the sensitivity of our frequency measurement.
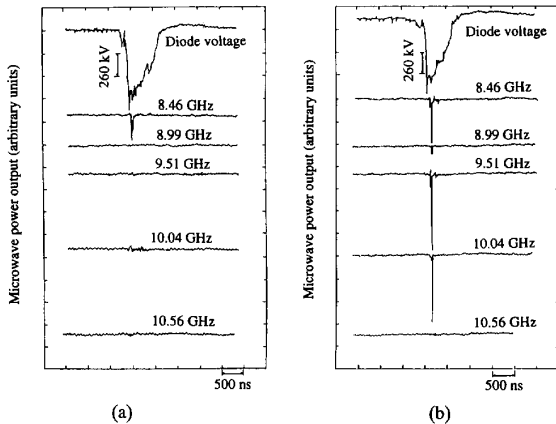

Fig. 6. Oscilloscope traces from the microwave spectrometer and the beam voltage: (a) vacuum BWO, (b) plasma filled BWO (60 mT, $I = 3$ kA). The center frequency of each channel is indicated.

of the background helium pressure is shown in Fig. 7. The percentage bandwidth $\Delta f / f_0$ changed from $\leq 5\%$ in vacuum to 25% at the pressure of maximum power enhancement. As shown in Fig. 6(b), rf pulse duration is shorter in the higher frequency channels, i.e., the pulse duration in channel 1 is about 30 ns, but is only 10 ns in channel 4.

With 3 kA of beam current injected into the helium-filled BWO, we observed microwave power enhancement for helium pressure between 10 mTorr to 100 mTorr, with maximum
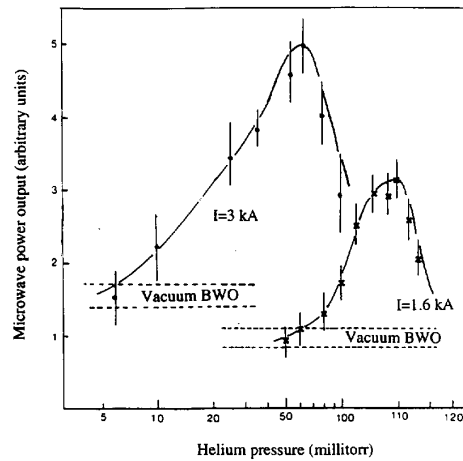

Fig. 8. Microwave power output vs background helium pressure for beam currents of 3 and 1.6 kA. Microwave output for the vacuum BWO is given by the dashed lines. The plasma density as a function of time for the $I = 1.6$ case can be found in Fig. 5.

power at 60 mT. When the beam current was reduced to 1.6 kA, the power enhancement began at ~ 80 mT, peaked at 110 mT, then declined. In Fig. 8, the output is the summation of all the signals from channel 1 to channel 4 of the spectrometer ($8.2 \leq f \leq 10.8$ GHz) while the vacuum BWO microwave power output (dashed line) was the signal from the first channel ($8.2 \leq f \leq 8.7$ GHz).
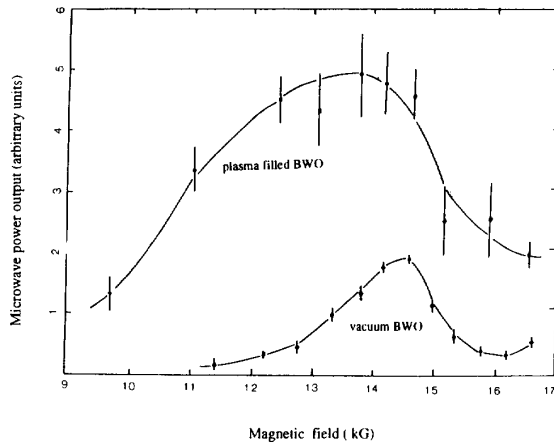
Fig. 9.   Microwave power output vs. guiding magnetic field in both vacuum and plasma-filled BWO's.

Microwave power depended on the guiding magnetic field, B, both for vacuum and plasma-filled BWO's (Fig. 9). In the plasma-filled BWO, we kept the background helium pressure in the maximum rf output range, e.g., at ~60 mTorr for the 3 kA beam current. Microwave power peaked around 13.5 kG, with a wider range compared to the vacuum BWO. The vacuum BWO peaked at a slightly larger B field ~14.5 kG. Our 13.5 kG field is much higher than the peak rf emission field (9–10 kG) reported in [2] in their helium-gas-filled BWO. We are not sure of the reason for this difference.

Overall, our BWO generated between 560 ~ 700 MW ($8.2 \leq f \leq 10.8$ GHz) microwave power with plasma, and $80 \sim 100$ MW ($8.2 \leq f \leq 8.725$ GHz) in vacuum. rf power enhancement appeared over a much wider pressure range for high beam currents than for the lower current driven BWO. Microwave frequency upshifted 1 GHz in the microwave power enhancement background helium pressure region for both 1.6 kA and 3 kA of beam current. This is less than the theory of [14], which predicts a 2.5 GHz upshift at $n_p = 8 \times 10^{11}$ cm^{-3} (Our plasma density measurements indicate $n_p \geq (8 \pm 1.5) \times 10^{11}$ cm^{-3}.) The background plasma increases the beam electron kinetic energy by reducing the space charge potential produced by the beam in the BWO. This will shift the beam wave intersection point up in frequency. However, a simple calculation based on the interaction of the uncoupled dispersion curve for the BWO and the electron beam yield a frequency upshift of less than 200 MHz for our electron beam parameters. Along with the frequency upshift, bandwidth increased with plasma density. Although the rf pulse duration decreased from 50 ns in vacuum to about 20 ~ 30 ns in plasma filled-BWO, this is not sufficient to account for the observed bandwidth increase.

B. T-G Modes in the Plasma-Filled BWO

Our second step was to look for rf emission (T–G modes) in the plasma-filled BWO, using the antenna placed in the ninth ripple of the BWO, and also using an S-band microwave horn at the end of the chamber. Broadband low frequency

microwave radiation was detected up to the plasma frequency of the background plasma. This appeared only with plasma in the BWO, at frequencies below the cutoff frequency of the plasma-filled BWO and lower than the plasma frequency f_p. Power and pulse duration depended on n_p. When the background helium pressure was lower than 70 mT ($n_p < 4 \times 10^{11}$ cm^{-3}, $f_p < 5.7$ GHz), there was no rf signal in the J-band spectrometer. rf appeared in every channel of the S-band spectrometer with about the same amplitude and pulse duration. The T–G mode emission ($f < 5.7$) GHz correlated with the X-band TM$_{01}$ mode emission. As in Fig. 10, T–G mode power emission always dropped when the TM$_{01}$ mode peaked. This mode competition appeared every shot for about 100 shots when $n_p < 4 \times 10^{11}$ cm^{-3}. As plasma density rose to 4×10^{11} cm^{-3} the TM$_{01}$ mode power output showed no change. However, the T–G mode emission power gradually increased by a factor of 2 over a plasma density change of 2 to 4×10^{11} cm^{-3} (4 GHz$< f_p < 5.7$ GHz). As the pressure reached 100 mT ($n_p \sim 7 \times 10^{11}$ cm^{-3}, $f_p = 7.5$ GHz), rf signals appeared in the first seven channels of the J-band spectrometer (eighth channel overlapped with the X-band TM$_{01}$ emission) and every channel of the S-band spectrometer. The S and J-band spectrometer signals lasted ~100 ns. Signals in J-band had smaller amplitude than that of the S-band. However, since we could not determine the coupling efficiency of the antenna as a function of frequency, and the presence of the S-band waveguide (Fig. 3), we cannot determine quantitative differences in S and J-band signals.

As the background helium pressure reached 120 mT ($n_p = n_{cr} \sim 8 \times 10^{11}$ cm^{-3}, $f_p \sim 8$ GHz) a simultaneous peak in the TM$_{01}$ mode and the T–G modes (both S and J-band) was observed (Fig. 10(c)). A sudden enhancement appeared in the S-band T–G mode peak power of up to 8 dB. The J-band rf signal amplitude increased with the S-band rf but no more than 3 dB. The X-band TM$_{01}$ mode emission increased for 6×10^{11} cm$^{-3} < n_p < 8 \times 10^{11}$ cm^{-3} and peaked at n_{cr}. Power enhancement was typically a factor of 3 at n_{cr}, but up to a factor of 6 in some shots. This enhancement in X-band TM$_{01}$ mode radiation for plasma filled BWOs has been observed by others [9], [10]. Possible mechanism of the enhancement can be found in [18] and [19]. The correlation and enhancement of the T–G modes in a plasma filled BWO was discussed in [14].

Given the error in the plasma density measurement, the background plasma density could be as high as $n_p \sim 9.5 \times 10^{11}$ cm^{-3} ($f_p \sim 8.8$ GHz) when the TM$_{01}$ mode and T–G modes power emission are enhanced. This could indicate the possibility that part of the enhanced X-band signal came from T–G mode radiation. Although the absolute T–G modes power emission was not calibrated, when a 27dB (constant attenuation for $0 < f < 18$ GHz) attenuator was placed in series with the detector and the RG-9 cable, the X-band rf could still be detected in the eighth bin of the J-band spectrometer (7.9 GHz$< f < 8.2$ GHz) but not the lower frequencies of the band. This indicated that the power carried by the T–G modes emission (in J-band) was at least 27 dB less than the X-band TM$_{01}$ mode. For plasma density $n_p > 8 \times 10^{11}$ cm^{-3}, power emission in the TM$_{01}$ mode gradually decreased, and the T–G modes pulse became much
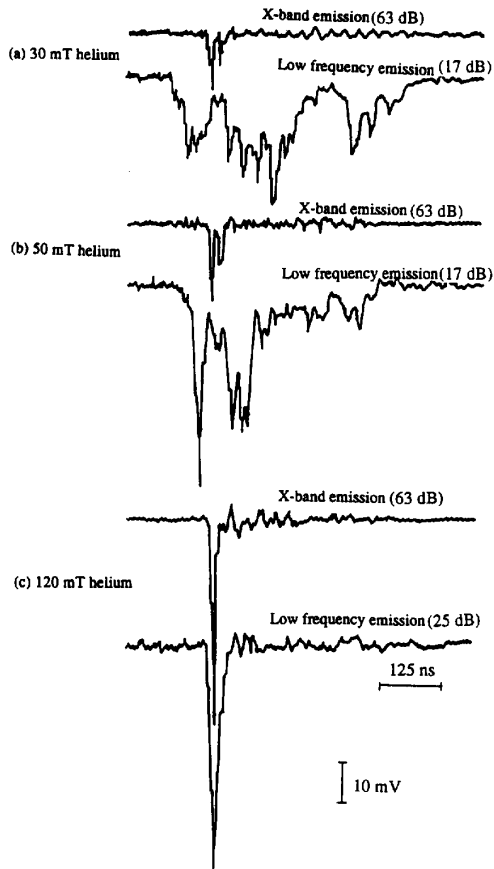
Fig. 10. Oscilloscope traces of the X-band (8.2–10.2 GHz, measured by X-band crystal detector) and the Trivelpiece–Gould modes (measured by a crystal detector) microwave signals. The low frequency emission was 2 GHz< f < 5.7 GHz, higher frequencies were cut off by an additional piece of RG-8 cable which attenuated rf at 0.7 dB/m at 4 GHz but 6 dB/m at 9 GHz. Frequencies less than 2 GHz were cut off by the S-band waveguide. The attenuation was kept the same for all cases except in the low frequency rf emission in (c), where an additional 8 dB was added. The background helium pressures were (a) 30 mT, (b) 50 mT, (c) 120 mT.
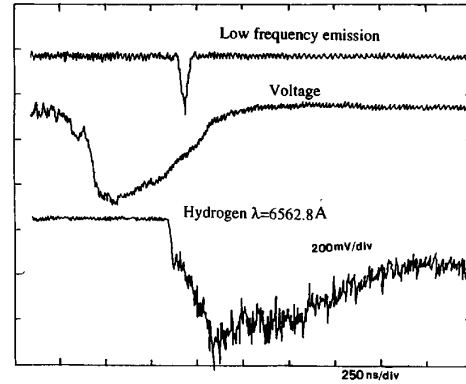

Fig. 11. Upper trace is the low frequency emission from the BWO without the background helium gas. Bottom trace is the light emission from wall plasma.

shorter ($\sim$50 ns) but their amplitude kept increasing (both S and J-band). When the pressure reached 170 mT the J and S-band power emission were 2–3 times larger than that of the 120 mT case. We were not able to measure the plasma density for background helium pressure higher than 130 mT, where $n_p \geq 10^{12}$ cm^{-3}, which was beyond the cutoff density for the 9.6 GHz magnetron rf.

To check that this low frequency emission was a result of the plasma present in the BWO, we tested without helium gas ("vacuum", 5×10^{-5} torr). We found broadband low frequency radiation with frequency 2.6 GHz< f < 5.85 GHz appeared very late (200 ns after the TM$_{01}$ rf signal turn off) in the beam pulse, when the beam voltage dropped to less than 200 kV. Nothing was detected in the J-band spectrometer. This puzzle was solved when we sought traces of Cu (wall material) and hydrogen atoms (water absorption on the BWO wall) with our optical spectroscopic system (Fig. 2). Measurements showed very strong hydrogen light from the BWO when the

low frequency radiation appeared (Fig. 11). Simultaneous Cu atomic emission was 20 times weaker than hydrogen radiation. We believe a hydrogen plasma forms from beam impact with adsorbed water, released by beam electrons hitting the BWO wall. The plasma density measurement showed this plasma density reached more than 10^{12} cm^{-3}, but came 200 ns later than the X-band radiation in the system. We also looked for T–G mode emission when we replaced the BWO with the tube of radius 10 mm. Broadband (2.6 GHz< f < 3.9 GHz, measured with the spectrometer and cut off filters) low frequencies emission was observed with amplitude ten times less than that of the plasma-filled BWO case. Also, emission in the smoothbore didn't appear until much later in the beam pulse, e.g., for 30 mT helium, low frequencies appeared 300 ns into the beam pulse, but in the plasma-filled BWO low frequencies started with the beam. Using the theory of [20], a calculation using cylindrical tube geometry indicates T–G modes with $v_{\text{phase}} = v_{\text{beam}}$ don't exist until $n_p \sim 2.9 \times 10^{12}$ cm^{-3} ($v_{\text{beam}} = 0.8c$ for $V = 400$ kV when T–G modes emission appeared). A gradient in plasma density of $\sim 3\%$ can account for the frequency spectrum. Our plasma density measurement showed that at 30 mT, n_p reached 10^{12} cm^{-3} about 300 ns after the beam started (see Fig. 5), consistent with the observed time of low frequency emission. At higher background gas pressure, the low frequency signals appeared much earlier in the beam pulse, because at higher pressure plasma density reached 2.9×10^{12} cm^{-3} much earlier.

In this part of the measurement, we measured broadband, low frequency microwaves in our plasma-filled BWO with a spectrum of 2.6 GHz< f < 7.85 GHz, without attempting to observe f < 2.6 GHz. We believe these waves arise from electron beam excitation of the "dense" spectrum of T–G modes discussed in [13], because at low helium pressure the low frequency emission from the plasma-filled BWO appeared as soon as the beam turned on, which we didn't see in the plasma-filled smoothbore case with the same gas pressure and beam current. Only in a plasma-filled BWO can one expect to see T–G modes with $v_{\text{phase}} = v_{\text{beam}}$ ($v_{\text{beam}} = 0.9c$ for $V = 650$ kV) when the plasma density is low. We also saw power increases of up to a factor of 2 in the broadband, low

frequency radiation ($f < 5.7$ GHz) when n_p rose from 2 to 4×10^{11} cm^{-3}. At $n_{cr} \sim 8 \times 10^{11}$ cm^{-3} a simultaneous and sudden enhancement in both the T–G ($f < 7.85$ GHz) and X-band output were observed. We are not sure why the low frequency in S-band of the T–G modes showed more power enhancement (up to 8 dB) at n_{cr} than that of the higher frequencies in J-band (only 3 dB). The exact mode structure of the T–G modes and the absolute power was not calibrated because of our limited diagnostic tools.

C. Electric Field Measurement

Using spectroscopic methods to measure electric field distributions in a relatively high noise level system is efficient and convenient. This method has been used in many laboratories [21]–[25] since Baranger and Mozer suggested in 1961 using the high-frequency Stark effect as a diagnostic tool to study the frequency and strength of the electrostatic fluctuations in a plasma [25]. We choose the four energy-level system (3^1P, 3^1D, 2^1P, 2^1S) of helium I for spectroscopic measurement. Transitions from 3^1P to 2^1S ($\lambda_A = 501.56$ nm) and from 3^1D to 2^1P ($\lambda = 667.80$ nm) are allowed, and the transition from 3^1P to 2^1P is forbidden ($\lambda_F = 663.20$ nm) in the electric dipole approximation. In a perturbing electric field, energy levels 3^1D and 2^1P are mixed; therefore, it is possible to see photons from the forbidden line. The perturbing electric field strength can be calculated [23] by the forbidden ($\lambda_F = 663.20$ nm) and allowed ($\lambda_A = 501.56$ nm) line intensity ratio (I_F/I_A):

$$E = 305.8 \left(\frac{I_F}{I_A} \right)^{0.54} \text{kV/cm}. \qquad (2)$$

In these studies we increased the diode A–K gap reducing the beam current to ~ 1 kA, to get a longer microwave pulse. Forbidden line photons appear with the high power microwave emission, while allowed line photons appear earlier and last much longer than the rf pulse (Fig. 12). This is because the forbidden transition only happens when there are electric fields in the system, while the allowed transition occurs as long as there is plasma, exciting the helium electrons to higher energy levels. This suggests that the electric fields inducing the forbidden transitions were produced by the high power rf. We counted photon numbers in each time interval for both the forbidden and allowed lines in each shot, then averaged over ~ 100 shots. The ratio of the average photon numbers in the forbidden and allowed lines was used to calculate the electric field with (2).

Fig. 13 shows the results of the electric field measurement in the plasma-filled BWO when the rf was enhanced by the background plasma by a factor of 2 over its vacuum counterpart. The measured rf power was 80 MW±10 MW and the rf pulse duration (FWHM) was ~ 60 ns. Fig. 13 shows the electric fields lasted only as long as the microwave pulse, peaking at 34 kV/cm, then dropping to ~ 12 kV/cm.

When the background plasma density was $\sim 10^{12}$ cm^{-3}, the X-band rf turned off. At the same time an rf signal appeared in Ku-band with center frequency of 14.6 GHz and ~ 150 ns pulse duration. This is the mode switching from the TM$_{01}$
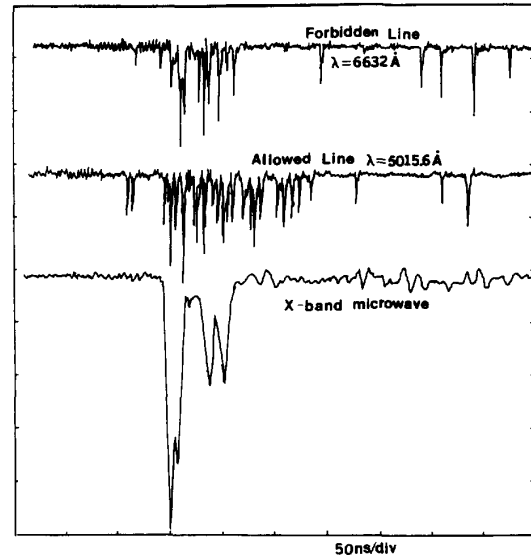

Fig. 12.   Oscilloscope trace of the forbidden and allowed line photons and the microwave pulse.
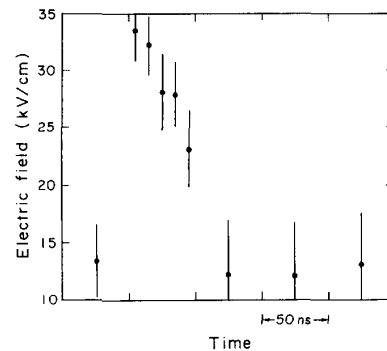

Fig. 13.   Electric field vs. time when the BWO rf power was enhanced by the background plasma.

mode to the TM$_{02}$ mode in the plasma-filled BWO, as reported and discussed in [14]. Electric fields present in the plasma filled BWO were measured when the mode switching occurred. The measured electric field strength after mode switching was about 16 kV/cm (Fig. 14) and lasted 150 ns, as long as the TM$_{02}$ microwave pulse.

To estimate how much microwave power this field strength implies, assume a smooth wall tube with radius of $R_0 = 1.9$ cm (this measurement was done in the wide part of the BWO where $r = 1.9$ cm). Assuming a TM$_{0n}$ mode propagating along the axis, we have

$$S = \frac{c}{8\pi} \frac{1}{\sqrt{\mu\epsilon}} \left(\frac{\omega}{\omega_{\lambda n}} \right)^2 \sqrt{\left(1 - \frac{\omega_{\lambda n}^2}{\omega^2} \right)}$$
$$\cdot E_0^2 \int_0^{R0} \left[J_0 \left(\frac{\gamma_{0n} r}{R_0} \right) \right]^2 2\pi r \, dr. \qquad (3)$$

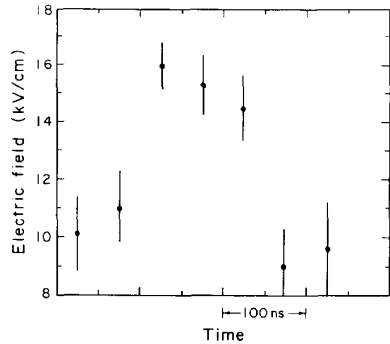Here S is the power flux of the rf in the tube, with $\omega/2\pi = 9.5$ GHz, the center rf frequency of the plasma-

Fig. 14. Electric field vs. time when mode switching occurred.

filled BWO, γ_{0n} is the nth root of $J_0(r)$, and $\omega_{\lambda n}$ is the cut-off frequency of the tube for the TM_{0n} mode, and E_0 is the amplitude of the electric field. The quantity we measured is $\overline{E} = \sqrt{\langle E^2 \rangle} = 34$ kV/cm. To get E_0^2 we have:

$$E_0 = 1.41\sqrt{\langle E^2 \rangle}. \qquad (4)$$

For the TM_{01} mode, (3) and (4) give $S = 19\pm 11$ MW, with the uncertainty due to the 30% error in electric field measurement. Direct microwave power measurement gives 80 MW$\pm$10 MW.

This 34 kV/cm electric field is lower than we expected from the direct rf power measurement, since it gives a power flux lower than the measured X-band microwave power and there were other waves (Trivelpiece–Gould modes) in the plasma-filled BWO which contribute to $\overline{E}$. Although the Trivelpiece–Gould mode had 20 dB less power than the X-band TM_{01}, it could produce electric fields ~ 1 kV/cm. Using the same method as for the TM_{01} mode, we estimated that the TM_{02} mode rf power emission was only 0.3 MW. Some error may come from the assumption of a TM_{0n} mode propagating axially in a 19 mm radius smooth tube with a average electric field the same as our measured field value. The actual measurement was done in a rippled wall BWO. In a BWO, the electric field distribution of a TM_{0n} mode peaks near the BWO wall rather than on the axis. To accurately calculate the power flux in the BWO, one has to know the electric field distribution $\vec{E}(\vec{r})$ in the BWO and the light collecting efficiency as a function of position in the BWO, a very complex calculation. We have not done this calculation at this time. The electric field from the electron beam charge is not important here. For the 1 kA beam the beam density is $\sim 5 \times 10^{11}$ cm^{-3} whereas n_p was as high as 8×10^{11} cm^{-3} when the rf pulse appeared and the electric field peaked. Therefore, the beam was charge neutralized.

IV. CONCLUSION

In conclusion, we have observed microwave frequency upshifts of up to 1 GHz and a bandwidth increase from ≤ 0.5 GHz to 2 GHz along with an enhancement by a factor of 7 in the total microwave power emission in our plasma filled BWO. We also measured T–G modes with frequencies up to the background plasma frequency in our plasma-filled BWO. This

could be the "dense spectrum" of plasma waves as discussed in [13]. At a critical plasma density the T–G modes and the BWO TM_{01} mode output power were simultaneously enhanced. The T–G mode measurement and the electric field measurement, to the best of our knowledge, have not been done previously for a device of this kind. In the plasma filled BWO, we measured the average electric field strength as a function of time on our BWO axis, where the relativistic electron beam, high power microwaves and plasma interact. While the microwave power output was enhanced by the background plasma, the electric field peaked at 34 kV/cm and lasted only as long as the high power rf pulse, about 50 ns.

REFERENCES

[1] J. A. Nation, "On the coupling of an high-current relativistic electron beam to a slow wave structure," *Appl. Phys. Lett.*, vol. 17, no. 11, pp. 491–494, Dec. 1970.
[2] Y. Carmel, J. Ivers, R. E. Kribel, and J. Nation, "Intense coherent Cherenkov radiation due to the interaction of a relativistic electron beam with a slow-wave structure," *Phys. Rev. Lett.*, vol. 33, no. 12, pp. 1278–1282, July 1974.
[3] M. Friedman, "Emission of intense microwave radiation from an auto-modulated relativistic electron beam," *Appl. Phys. Lett.*, vol. 26, no. 7, pp. 366–368, April 1975.
[4] V. I. Belousov, V. V. Bunkin, A. V. Gaponov-Grekhov et al., "Intense microwave emission from periodic relativistic electron bunches," *Sov. Tech. Phys. Lett.*, vol. 4, no. 12, pp. 584–585, Dec. 1978.
[5] V. S. Ivanov, N. F. Kovalev, S. I. Krementsov, and M. D. Raizer, "Relativistic millimeter carcintron," *Sov. Tech. Phys. Lett.*, vol. 4, pp. 329–330, July 1978.
[6] N. I. Zaitsev, N. F. Kovalev, G. S. Korablev, I. S. Kulagin, and M. M. Ofitserov, "Relativistic carcinotron with $\lambda = 3$ cm and pulse length of 0.4 μs," *Sov. Tech. Lett.*, vol. 7, no. 7, pp. 477–378, July 1981.
[7] Yu. F. Bondar', S. I. Zavorotnyi, A. L. Ipatov, N. I. Karbushev, N. F. Kovalev, O. T. Loza, G. P. Mkheidze, and L. E' Tsopp, "Measurement of rf emission from a carcinotron with a relativistic electron beam," *Sov. J. Plasma Phys.*, vol. 9, no. 2, pp. 223–226, March–April 1983.
[8] V. S. Ivanov, S. I. Krementsov, V. A. Kutsenko, M. D. Raizer, A. A. Rukhadze, and A. V. Fedotov, "Investigation of a relativistic Cerenkov self-generator," *Sov. Phys. Tech. Phys.*, vol. 26, no. 5, pp. 580–583, May 1980.
[9] Yu. V. Tkach, Ya. B. Fainberg, I. I. Magda, N. I. Gaponenko, G. V. Skachek, S. S. Pushharev, N. P. Gadetskii, and A. A. Belukha, "Microwave emission in the interaction of a high-current relativistic beam with a plasma-filled slow-wave structure," *Sov. J. Plasma Phys.*, vol. 1, no. 1, pp. 43–46, Jan.–Feb. 1975.
[10] Y. Carmel, K. Minami, R. A. Kehs, W. W. Destler, V. L. Granatstein, D. Abe, and W. L. Lou, "Demonstration of efficiency enhancement in a high-power backward-wave oscillator by plasma injection," *Phys. Rev. Lett.*, vol. 62, no. 20, pp. 2389–2492, May 1989.
[11] X. Zhai, E. Garate, R. Prohaska and G. Benford, "Study of an X-band backward wave oscillator," *Appl. Phys. Lett.*, vol. 60, no. 19, pp. 2332–2334, May 1992.
[12] A. W. Trivelpiece et al., "Space charge wave in cylindrical plasma columns," *J. Appl. Phys.*, vol. 30, no. 11, pp. 1784–1793, Nov. 1959.
[13] W. R. Lou, Y. Carmel, W. W. Destler, and V. L. Granatstein, "New mode in a plasma with periodic boundaries: the origin of the dense spectrum," *Phys. Rev. Lett.*, vol. 67, no. 18, pp. 2481–2484, Oct. 1991.
[14] Y. Carmel, K. Minami, W. R. Lou, R. A. Kehs, W. W. Destler, V. L. Granatetein, D. K. Abe, and J. Rodgers, "High-power microwave generation by excitation of a plasma-filled rippled boundary resonator," *IEEE Trans. Plasma Sci.*, vol. 18, pp. 497–506, June 1990.
[15] X. Zhai, E. Garate, R. Prohaska, and G. Benford, "Observation of Trivelpiece–Gould modes in a plasma-filled backward wave oscillator," *Phys. Rev. A*, vol. 45, no. 12, pp. 8336–8339, June 1992.
[16] K. Minami, Y. Carmel, V. L. Granatstein, W. W. Destler, W. R. Lou, D. K. Abe, R. A. Kehs, M. M. Ali, T. Hosokawa, K, Ogura, and

T. Watanabe, "Linear theory of electromagnetic wave generation in a plasma-loaded corrugated-wall resonator," *Plasma Sci.*, vol. 18, pp. 537–544, June 1990.

[17] K. Minami, W. R. Lou, W. W. Destler, R. A. Kehs, V. L. Granatsein, and Y. Carmel, "Observation of a resonant enhancement of microwave radiation from a gas-filled backward wave oscillator," *Appl. Phys. Lett.*, vol. 53, no. 7, pp. 559–561, May 1988.

[18] A. T. Lin and L. Chen, "Plasma-induced efficiency enhanced in a backward-wave oscillator," *Phys. Rev. Lett.*, vol. 63, no. 26, pp. 2808–2811, Dec. 1989.

[19] M. Botton and Amiran Ron, "Efficiency enhancement of a plasma filled backward-wave oscillator by self-induced distribution feedback," *Phys. Rev. Lett.*, vol. 66, no. 19, pp. 2468–2471, May 1991.

[20] E. P. Garate, A. Fisher, and W. Main, "High-gain plasma Cerenkov maser," *IEEE J. Quantum Electronics*, vol. 25, no. 7, pp. 1712–1719, Jul. 1989.

[21] A. Dovrat and G. Benford, "Optical diagnosis of electric fields in a beam-driven turbulent plasma," *Phys. Fluids B*, vol. 1, no. 12, pp. 2488–2491, Dec. 1989.

[22] H. -J. Kunze and H. R. Griem, A. W. DeSilva, G. C. Goldenbaun, and I. J. Spalding, "Spectroscopic investigation of enhanced plasma oscillation in a high-voltage theta pinch," *Phys. Fluids*, vol. 12, no. 12, pp. 2669–2676, Dec. 1969.

[23] K. Kawasaki, T. Usui, and T. Oda, "Forbidden transition in helium and lithium due to fluctuating electric field for plasma diagnostics," *J. Phys. Soc. Jpn*, vol. 51, pp. 3666–3671, May 1982.

[24] G. C. A. M. Janssen, E. H. A. Granneman, and H. J. Hopman, "Observation of high-frequency fields due to the interaction of a relativistic electron beam with a plasma," *Phys. Fluids*, vol. 27, no. 3, pp. 736–745, March 1984.

[25] M. Baranger and B. Mozer, "Light as a plasma probe," *Phys. Rev.*, vol. 123, no. 1, pp. 25–28, Feb. 1961.

Xiaoling Zhai, photograph and biography not available at the time of publication.

Eusebio Garate, photograph and biography not available at the time of publication.

Robert Prohaska, photograph and biography not available at the time of publication.

Gregory Benford, photograph and biography not available at the time of publication.

Amnon Fisher (M'86) photograph and biography not available at the time of publication.